Specific Inclusion Mode of Guest Compounds in the Amylose Complex Analyzed by Solid State NMR Spectroscopy

Yuichi TOZUKA,*[,a] Aya TAKESHITA,[a] Ayako NAGAE,[a] Arpansiree WONGMEKIAT,[a] Kunikazu MORIBE,[a] Toshio OGUCHI,[b] and Keiji YAMAMOTO[a]

[a] *Graduate School of Pharmaceutical Sciences, Chiba University; 1–33 Yayoi-cho, Inage-ku, Chiba 263–8522, Japan: and* [b] *Department of Pharmacy, University Hospital, University of Yamanashi; 1110 Shimokato, Tamaho-cho, Chuo, Yamanashi 409–3898, Japan.*

Received February 1, 2006; accepted May 3, 2006; published online May 19, 2006

The inclusion compound formation between linear amylose of molecular weight 102500 (AS100) and *p*-aminobenzoic acid (PA) during the sealed-heating process was investigated by powder X-ray diffractometry, infrared spectroscopy and solid state NMR spectroscopy. Sealed-heating of AS100 and PA at 100 °C for 6 h provided an inclusion compound with 6_1-helix structure, while a 7_1-helix structure was found when sealed-heating was carried out at 150 °C for 1 h. The formation of an inclusion compound was not observed when sealed-heating was performed at 50 °C for 6 h. The 7_1-helix inclusion compound maintained its structure even during storage at high temperature while the 6_1-helix inclusion compound decomposed and returned to the original V_a-amylose upon heating to 180 °C. Quantitative determination revealed that one PA molecule could be included per one helical turn of AS100 for both 6_1-helix and 7_1-helix inclusion compounds. Solid state NMR spectroscopy suggested that PA molecules were included in the amylose helix core in the 7_1-helix inclusion compound, while in the case of 6_1-helix inclusion compound, PA molecules were accommodated in the interstices between amylose helices. Moreover, the inclusion compound formation by sealed-heating of AS100 was also observed when using PA analogues as guest compounds. The binding ratio of AS100 and PA analogues varied depending on the size of guest molecules.

Key words amylose; *p*-aminobenzoic acid; sealed-heating; inclusion compound; solid state NMR; molecular mobility

Amylose is a polysaccharide consisting of α-1,4-linked D-(+)-glucopyranoses which take three helical forms, namely; A-, B-, and V-amyloses.[1,2] A- and B-structures are found in native amyloses with a double helix, while the V-structure is formed at inclusion compound formation with a complexing ligand. Several kinds of guest compounds can be included in the hydrophobic core of V-amylose and normally V-amylose takes a single helical structure with 6 glucose units per turn (6_1-helix).[3—6] However, when amylose adopts larger guests, the structure of V- are found to be a 7_1-helix[7—9] or 8_1-helix[10—12] depending on the size of guest molecules. The inclusion compounds are usually prepared from aqueous solution of amylose by adding an alcoholic solution of guest compound.

The sealed-heating method can be used to prepare inclusion compounds of cyclodextrin.[13—15] Previously we have applied the sealed-heating method for the preparation of amylose inclusion compounds with several guest molecules.[16—19] Salicylic acid analogues,[16,17] benzoic acid analogues[18] and 2-naphthol[19] are examples of guest molecules that could form inclusion compound with amylose by the seal-heating method. We also reported that the vapor pressure of the guest and the water content in the sealed-heating process were significant factors for the formation of inclusion compound.[16,17] Powder X-ray diffraction and infrared spectroscopy were used to investigate the interaction between amylose and guest molecules.

In the present study, we prepared the inclusion compound between amylose and PA by sealed-heating method. Since the powder X-ray diffraction patterns provide only the structure change of amylose, solid state NMR spectroscopy was used in order to estimate the molecular state and molecular mobility of PA in the inclusion compound. The effect of heating temperature and the size of guest molecules on the inclusion compound formation were also investigated.

Experimental

Materials Linear amylose of molecular weight 102500 (AS100) was kindly supplied by Ezaki Glico Co., Ltd. The particle size of AS100 was controlled between 42.5 and 150 μm by sieving. *p*-Aminobenzoic acid (PA), methyl *p*-aminobenzoate (MPA), ethyl *p*-aminobenzoate (EPA), butyl *p*-aminobenzoate (BPA) were purchased from Nakalai Tesque, Japan. Propyl *p*-aminobenzoate (PPA) was obtained from Tokyo Kasei Kogyo Co., Ltd. All chemicals were of reagent grade.

Sample Preparation and Sealed-Heating Procedure A physical mixture was prepared at a mixing ratio of 1 : 1 and 1 : 2 (6 glucose units: PA) in a glass vial for 5 min using a vortex mixer. As a pretreatment, AS100 was dried at 100 °C for 3 h and then humidified at 33% relative humidity at 25 °C for 1 d before use. The water content of AS100 after humidification was determined by the Karl–Fischer method and was estimated to be 8.0%. A physical mixture (200 mg) was sealed in a 2 ml glass ampoule and then heated at various temperatures for a definite time.

Powder X-Ray Diffractometry Powder X-ray diffraction (PXRD) was performed using a Rigaku Miniflex diffractometer (Rigaku Corporation, Japan). The measurement conditions were as follows: target, CuK_α; filter, Ni; voltage, 30 kV; current, 15 mA; scanning range, 5—35°; scanning speed, 4°/min. Varied temperature powder X-ray diffraction (VXRD) was carried out on Phillips X'Pert-MPD PW3050 (Netherlands) equipped with a Phillips Japan TTK2-HC heat controller attachment model (Japan). The measurement conditions were as follows: target, CuK_α; filter, graphite monochromator; voltage, 40 kV; current, 50 mA; scanning range, 5—35°; scanning speed, 0.1°/min; heating rate, 5 °C/min.

Fourier-Transformed Infrared (FT-IR) Spectroscopy Fourier-transformed infrared spectra were determined by the KBr disc method using a JASCO FT/IR-230 spectrophotometer (Japan Spectroscopy Co., Ltd., Japan).

Solid State ^{13}C-NMR Spectroscopy ^{13}C-NMR spectra were determined on a JNM-LA400 NMR spectrometer (JEOL, Japan) operating with a CP/MAS (cross-polarization/magic angle spinning) or PST/MAS (pulse saturated transfer/magic angle spinning) probe. The sample was filled in a cylindrical rotor and spun at 6000 Hz. The measurement conditions were as follows: contact time, 5 ms; repetition time, 30 s; spectral width, 40 kHz; number of data points, 32756; number of accumulations, 8720 times.

* To whom correspondence should be addressed. e-mail: ytozuka@p.chiba-u.ac.jp

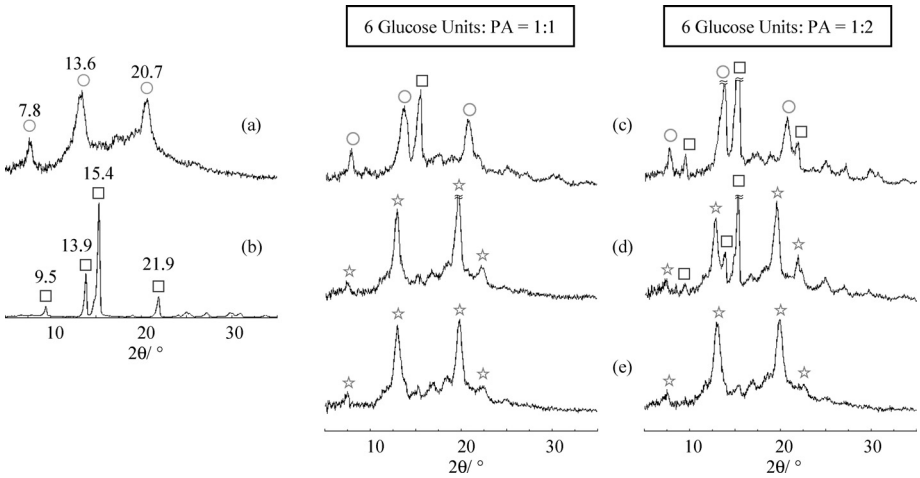

Fig. 1. Changes in PXRD Patterns of AS100-PA Systems by Sealed-Heating at 100 °C for 6 h

(a) AS100, (b) PA, (c) physical mixture, (d) sealed-heated sample, (e) after storage of (d) in a vacuum at 100 °C for 1 h. □: PA, ○: 6_1-helix V_a-type, ☆: 6_1-helix V_h-type.

Solid State ^{1}H-NMR Spectroscopy ^{1}H-NMR spectra were determined on a JNM-CMN NMR spectrometer (JEOL, Japan) by CRAMPS (combined rotation and multiple pulse spectroscopy) method. The measurement conditions were as follows: sample spinning, 1200 Hz; repetition time, 30 s; spectral width, 10 kHz; number of data points, 8192; number of accumulations, 256 times.

Determination of Included Amount of Guest Compounds To remove guest compound not included, sealed-heated samples were stored in a vacuum at 100 °C for 1 h. Treated samples were then dispersed into JP 2nd fluid and sonicated for 30 min. After filtration through a 1.0-μm membrane filter, the guest concentration in each solution was determined spectrophotometrically at 265.0, 284.6, 284.0, 284.4 and 285.6 nm for PA, MPA, EPA, PPA and BPA, respectively using Shimadzu UV-160 spectrophotometer.

Results and Discussion

Physical mixtures of AS100 and PA at mixing ratios of 1 : 1 and 1 : 2 (6 glucose units: PA) were sealed-heated at 100 °C for 6 h and the PXRD patterns of the samples are shown in Fig. 1. Crystalline *p*-aminobenzoic acid exhibits sharp crystalline peaks at 2θ=9.5, 13.9, 15.4 and 21.9°. AS100 shows rather broad diffraction peaks at 2θ=7.8, 13.6 and 20.7° due to the 6-helix structure of anhydrous V-amylose (V_a-amylose). After the sealed-heating of the 1 : 1 physical mixture, new diffraction peaks at 2θ=7.3, 12.9, 19.7 and 22.3° were observed, while the characteristic diffraction peaks of PA and anhydrous V-amylose disappeared. The newly observed diffraction peaks are the same as those of 6_1-helix V-amylose hydrate (V_h-amylose), suggesting that the formed compound between AS100 and PA has a similar structure to 6_1-helix V_h-amylose. In the 1 : 2 system, the PXRD peaks due to PA crystals were still observed in the sealed-heated sample with the newly observed peaks; the peaks of PA crystals disappeared after the storage of the sample in a vacuum at 100 °C for 1 h. Finally, the PXRD patterns coincided with the sealed-heated 1 : 1 mixture.

Fourier-transformed IR spectroscopy was used to investigate the molecular state of PA in the sealed-heated samples. Figure 2 demonstrates the changes in IR spectra of the AS100 : PA 1 : 1 and 1 : 2 (6 glucose units: PA) systems. The physical mixtures show an absorption band around 1661—1663 cm^{-1} due to the carbonyl stretching vibration of PA molecules. A shift of the absorption band to 1672 cm^{-1} is observed in the sealed-heated samples, which is considered to be due to the formation of hydrogen bonding between the

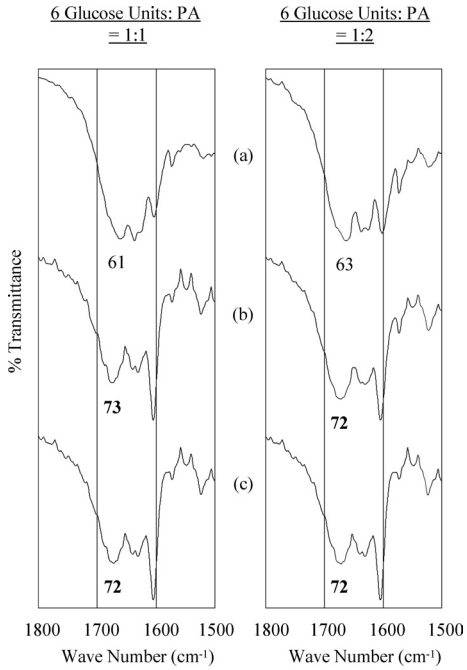

Fig. 2. Changes in IR Spectra of AS100-PA Systems by Sealed-Heating at 100 °C for 6 h

(a) Physical mixture, (b) sealed-heated sample, (c) after storage of (b) in a vacuum at 100 °C for 1 h.

carbonyl group of PA and the hydroxyl group of AS100. The results of PXRD and IR indicate the formation of an inclusion complex between PA and AS100.

The amount of PA included in AS100 was quantitatively determined. The sealed-heated samples were stored in a vacuum at 100 °C for 1 h to remove excess free guest molecules and then the treated samples were dispersed into JP 2nd fluid. Since both AS100 and PA could dissolve in JP 2nd fluid, the amount of PA dissolved in the media was considered to be the amount of PA included in AS100. The results reveal that one PA molecule can be included per one helical turn of AS100 stoichiometrically either in 1 : 1 or 1 : 2 (6 glucose units: PA) systems.

The influence of the sealed-heating temperature and duration on the inclusion compound formation of AS100 and PA

at a mixing ratio of 1 : 1 (6 glucose units: PA) was investigated. The inclusion compound did not appear to form on sealed-heating at 50 °C for 6 h, since there were no changes in the PXRD pattern of sealed-heated sample (Fig. 3b). On the contrary, new diffraction peaks at 2θ=6.8, 13.0 and 18.1°, which the identical diffraction angles as 7_1-helix amylose, were observed in the sample sealed-heated at 150 °C for 1 h (Fig. 3d). Sealed-heating of AS100 and PA at 100 °C for 6 h resulted in the formation of an inclusion compound with $6_1(V_h)$-helix structure, while 7_1-helix structure was formed when sealed-heating was carried out at 150 °C for 1 h. Consequently, sealed-heating condition has a significant influence on the inclusion compound formation and also on the helical structure of amylose in the inclusion compound. Varied temperature X-ray diffraction (VXRD) was employed to investigate the physicochemical stability of the inclusion compound. The PXRD patterns and the percentage of PA remaining after heating at different temperatures for two types of inclusion compounds are shown in Fig. 4. In the case of $6_1(V_h)$-helix inclusion compound, the gradual change in PXRD patterns from V_h-amylose to V_a-amylose was observed upon heating. The percentage of PA remaining in the inclusion compound decreased with the increase heating temperature of 60—100 °C. The results imply that the structure of the $6_1(V_h)$-helix inclusion compound dissociates on sublimation of the guest molecules. At the same time the structure changes from V_h-amylose type to the original V_a-amylose type. On the other hand, the 7_1-helix inclusion compound exhibits good stability against heating since no significant changes occurred in the PXRD patterns and the percentage of PA remaining after heating remains high. The results suggest that PA associates more strongly to amylose helices in the 7_1-helix inclusion compound.

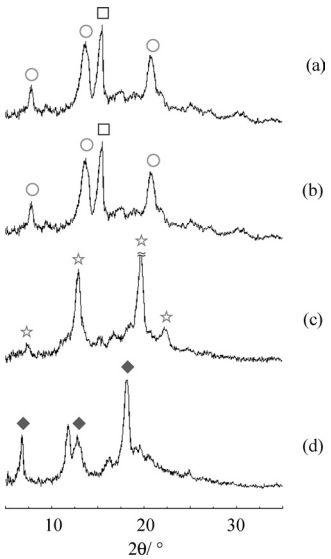

Fig. 3. Changes in PXRD Patterns of AS100-PA Systems by Sealed-Heating at Various Temperatures (6 Glucose Units: PA=1 : 1)

(a) Physical mixture, sample sealed-heated at (b) 50 °C for 6 h, (c) 100 °C for 6 h, (d) 150 °C for 1 h. □: PA, ○: 6_1-helix V_a-type, ☆: 6_1-helix V_h-type, ◆: 7_1-helix amylose.

Solid state NMR was employed to clarify the molecular state of PA in the inclusion compounds. Figure 5 shows the expanded region of solid state ^{13}C CP/MAS NMR spectra of AS100-PA (6 glucose units: PA=1 : 1) system. The $6_1(V_h)$-helix inclusion compound showed superimposed NMR signals of PA crystals and AS100. For PA crystals and the $6_1(V_h)$-helix inclusion compound, the resonance of C2′, C4′ and C6′ cannot be discriminated from each other since the

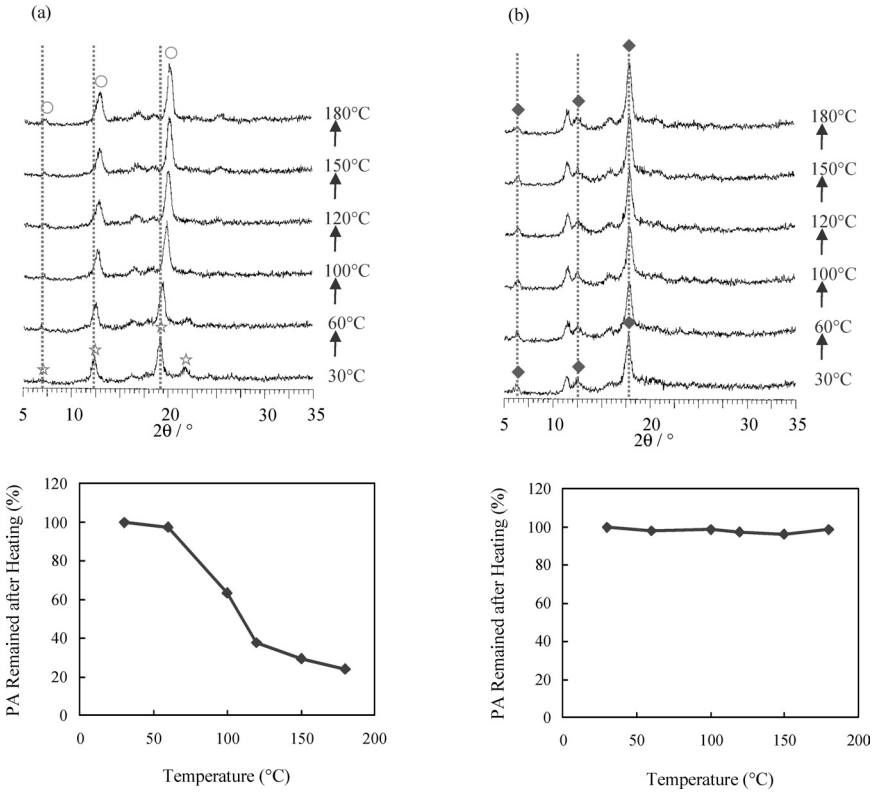

Fig. 4. Changes in PXRD Patterns as a Function of Temperature and Percentage of PA Remaining after Heating (Heating Rate: 5 °C/min)

(a) $6_1(V_h)$ helix inclusion compound, (b) 7_1-helix inclusion compound.

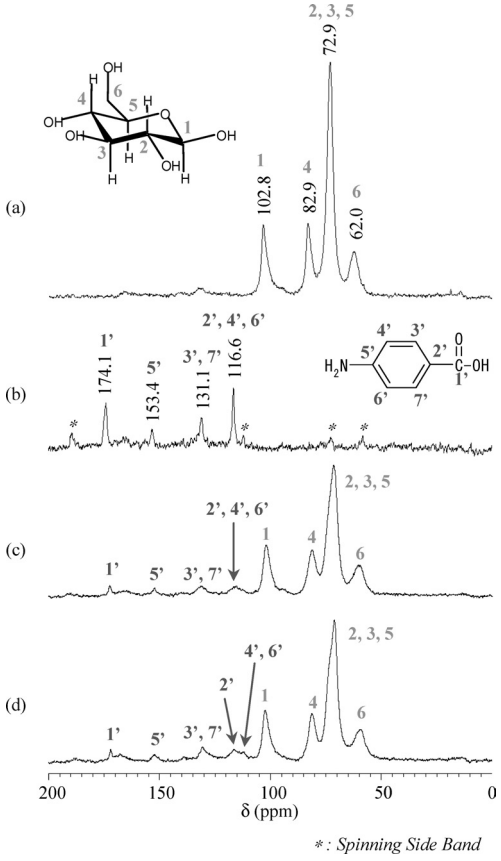

Fig. 5. Solid State ^{13}C CP/MAS NMR Spectra of AS100: PA (6 Glucose Units: PA = 1 : 1) System

(a) AS100, (b) PA, (c) $6_1(V_h)$-helix inclusion compound, (d) 7_1-helix inclusion compound.

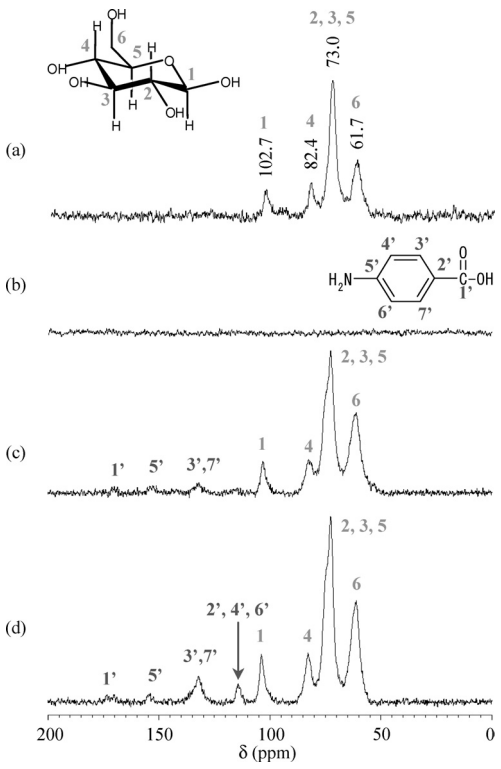

Fig. 6. Solid State ^{13}C PST/MAS NMR Spectra of AS100: PA (6 Glucose Units: PA = 1 : 1) System

(a) AS100, (b) PA, (c) $6_1(V_h)$-helix inclusion compound, (d) 7_1-helix inclusion compound.

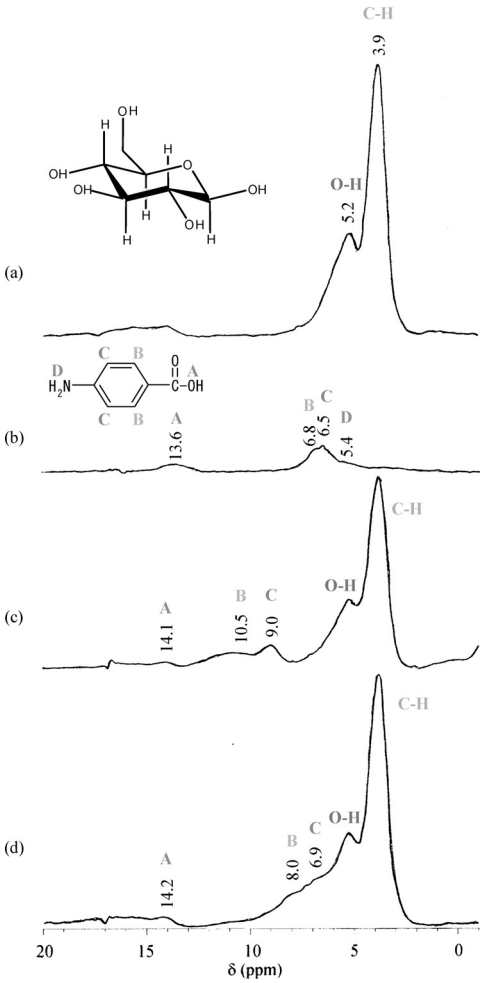

Fig. 7. Solid State ^1H CRAMPS NMR Spectra of AS100: PA (6 Glucose Units: PA = 1 : 1) System

(a) AS100, (b) PA, (c) $6_1(V_h)$-helix inclusion compound, (d) 7_1-helix inclusion compound.

resonance peaks appear as single peak. However, in the case of the 7_1-helix inclusion compound, this resonance peak separates into two peaks (originating from C2′ and C4′, 6′). The results suggested that the magnetic environment around benzene ring of PA was in a different state in the 7_1-helix inclusion compound compared to that in the $6_1(V_h)$-helix inclusion compound, which implies that PA molecules are included in a different manner in each inclusion compound.

To evaluate the molecular state of PA from the molecular mobility, solid state ^{13}C PST/MAS NMR spectroscopy was carried out. The ^{13}C PST/MAS NMR spectrum of PA crystals shows no peaks because PA molecules in the crystal lattice have low mobility (Fig. 6). Resonance peaks of the benzene carbons of PA can be observed more clearly in the spectrum of the 7_1-helix inclusion compound than in that of the $6_1(V_h)$-helix inclusion compound, indicating higher molecular mobility of PA in the 7_1-helix inclusion compound. A shift of the peak due to carbonyl C1′ from 174 to 170—172 ppm was observed in the case of the 7_1-helix inclusion compound. Moreover, the ^1H chemical shifts in the solid-state ^1H CRAMPS NMR spectra are observed for both of the inclusion compounds: PA carboxyl group (A) and benzene ring (B and C) as shown in Fig. 7. It is remarkable that, in the $6_1(V_h)$- or 7_1-helix inclusion complexes, the B and C proton

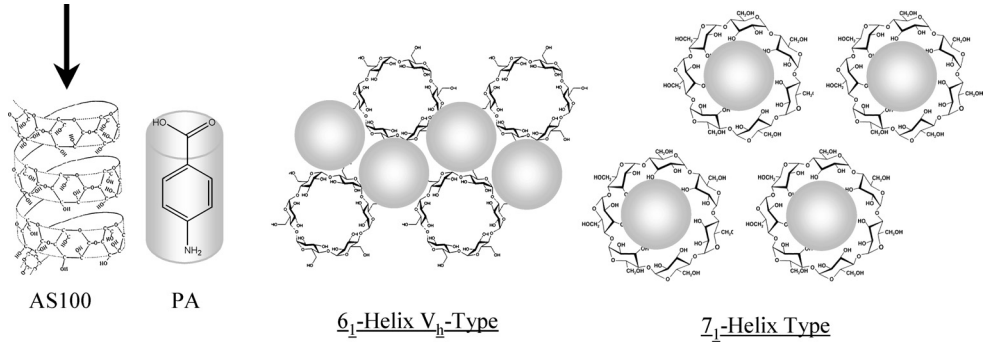

Fig. 8. Proposed Structure of AS100-PA Inclusion Compounds

Table 1. Calculated Stoichiometry of Amylose-Guest Inclusion Compounds

Guest	Binding ratio of guest to $6_1(V_h)$-helix amylose	Binding ratio of guest to 7_1-helix amylose
p-Aminobenzoic acid	1.0[a)]	0.9[d)]
Methyl *p*-aminobenzoate	1.0[a)]	1.0[d)]
Ethyl *p*-aminobenzoate	0.5[b)]	0.4[d)]
n-Propyl *p*-aminobenzoate	0.5[c)]	0.5[e)]
n-Butyl *p*-aminobenzoate	0.5[b)]	0.5[d)]

a) 100 °C · 6 h, *b*) 70 °C · 6 h, *c*) 90 °C · 6 h, *d*) 150 °C · 1 h, *e*) 150 °C · 5 h.

signals of PA appear downfield compared with the corresponding proton signals of PA crystals. The differences in the ^{1}H chemical shifts of PA between $6_1(V_h)$- and 7_1-helix inclusion complexes indicate a difference in the magnetic surroundings of PA molecules, which is supported by the difference in the ^{13}C CP/MAS spectra. These results suggest that hydrogen bonds are formed between the carbonyl groups of PA and the hydroxyl groups of AS100 in the inclusion compounds. Further, PA molecules might be accommodated in a different manner between the $6_1(V_h)$-helix and the 7_1-helix inclusion compounds.

Winter *et al.* reported the formation of 8_1-helix inclusion compound between amylose and α-naphthol.[11)] It was found that α-naphthol molecules were included both intra- and inter-helices. Dimethyl sulfoxide also formed 8_1-helix inclusion compound with amylose and be included both intra- and inter-helices.[19)] Although there was no report for the existence of guest molecules in the interstices of 6_1-helix amylose, it is likely that PA molecules were included in the interstices between amylose helices in the $6_1(V_h)$-helix inclusion compound. In contrast, considering that PA in the 7_1-helical complex is entrapped more strongly, PA molecules could be accommodated in the amylose helices core for the 7_1-helix inclusion compound (Fig. 8).

Finally, the effect of guest size on the inclusion formation was studied using four kinds of PA analogues, *i.e.*, MPA, EPA, BPA, and PPA. The formation of inclusion compounds was observed at adequate sealed-heated conditions for each compound. The binding ratio of MPA to amylose were 1 : 1 (guest molecule: helical turn), while guest molecules with larger size, *i.e.*, EPA, BPA and PPA were included at a binding ratio of 1 : 2 (guest molecule: helical turn) (Table 1).

Conclusions

Sealed-heating of AS100 with PA resulted in the formation of two kinds of inclusion compounds of differing helical structure, namely; a 7_1-helix and a $6_1(V_h)$-helix. Interestingly, the helical structure of the inclusion compound was dependent to the sealed-heating temperature. The 7_1-helix inclusion compound exhibits better stability at high temperature than the $6_1(V_h)$-helix inclusion compound. Solid state NMR studies revealed that the molecular mobility of PA and the magnetic environment around benzene ring of PA is in a different state in the 7_1-helix inclusion compound compared to that in the $6_1(V_h)$-helix inclusion compound. It is suggested that PA molecules are entrapped within amylose helices in the 7_1-helix inclusion compound; while in the case of $6_1(V_h)$-helix inclusion compound, PA molecules are included in the spaces between amylose helices.

Acknowledgments We are thankful to Ezaki Glico Co., Ltd. for a generous gift of amylose. We also thank Dr. Koji Saito and his group at Advanced Technology Research Laboratories, Nippon Steel Corporation for use of their NMR instrument. This study was supported in part by a Grant-in-Aid for Scientific Research from the Ministry of Education, Culture, Sports, Science and Technology of Japan (17790029)

References

1) Buleon A., Colona P., Planchot V., Ball S., *Int. J. Biol. Macromol.*, **23**, 85—112 (1998).
2) Winter W. T., Sarko A., *Biopolymers*, **13**, 1447—1460 (1974).
3) Takeo K., Kuge T., *Agric. Biol. Chem.*, **33**, 1174—1180 (1969).
4) Hulleman S. H. D., Helbert W., Chanzy H., *Int. J. Biol. Macromol.*, **18**, 115—122 (1996).
5) Bail P. L., Bizot H., Ollivon M., Keller G., Bourgaux C., Buleon A., *Biopolymers*, **50**, 99—110 (1999).
6) Snape C. E., Morrison W. R., Maroto-Valer M. M., Karkalas J., Pethrick R. A., *Carbohydr. Polym.*, **36**, 225—237 (1998).
7) Yamashita Y., Hirai N., *J. Polym. Sci., Part A-2*, **4**, 161—171 (1966).
8) Takeo K., Kuge T., *Agric. Biol. Chem.*, **35**, 537—542 (1971).
9) Wulff G., Kubik S., *Carbohydr. Res.*, **237**, 1—10 (1992).
10) Yamashita Y., Monobe K., *J. Polym. Sci., Part A-2*, **9**, 1471—1481 (1971).
11) Winter W. T., Chanzy H., Putaux J. L., Helbert W., *Polym. Prepr.*, **39**, 703—708 (1998).
12) Winter W. T., Sarko A., *Biopolymers*, **13**, 1461—1482 (1974).
13) Nakai Y., Yamamoto K., Terada K., Watanabe D., *Chem. Pharm. Bull.*, **35**, 4609—4615 (1987).
14) Nakai Y., Yamamoto K., Oguchi T., Yonemochi E., *Chem. Pharm. Bull.*, **38**, 1345—1348 (1990).
15) Oguchi T., Kojima K., Watanabe D., Yonemochi E., Yamamoto K., *J. Pharm. Sci. Technol. Jpn.*, **56**, 92—102 (1996).
16) Oguchi T., Yamasato H., Limmatvapirat S., Yonemochi E., Yamamoto K., *J. Chem. Soc., Faraday Trans.*, **94**, 923—927 (1998).
17) Uchino T., Tozuka Y., Oguchi T., Yamamoto K., *J. Inclu. Phenom. Macrocyclic Chem.*, **43**, 31—36 (2002).
18) Uchino T., Tozuka Y., Choi W.-S., Oguchi T., Yamamoto K., *Yakuzaigaku*, **62**, 58—66 (2002).
19) Uchino T., Tozuka Y., Oguchi T., Yamamoto K., *J. Inclu. Phenom. Macrocyclic Chem.*, **39**, 145—149 (2001).